GHRS OBSERVATIONS OF THE LISM

JEFFREY L. LINSKY
JILA, University of Colorado, Boulder, CO 80309-0440 USA

Abstract. The GHRS has obtained high-resolution spectra of interstellar gas toward 19 nearby stars. These excellent data show that the Sun is located inside the Local Interstellar Cloud (LIC) with other warm clouds nearby. I will summarize the physical properties of these clouds and the three-dimensional structure of this warm interstellar gas. There is now clear evidence that the Sun and other late-type stars are surrounded by hydrogen walls in the upwind direction. The D/H ratio probably has a constant value in the LIC, $(1.6 \pm 0.2) \times 10^{-5}$, consistent with the measured values for all LIC lines of sight.

Key words: LISM, interstellar medium, deuterium

1. Comparison of LISM Science Objectives with the Instrument Capabilities of the GHRS

To study the kinematics, physical properties, and chemical composition of the warm gas in the local interstellar medium (LISM) one must use an ultraviolet spectrograph with high spectral resolution and signal/noise (S/N). High spectral resolution is needed to identify individual clouds, a term that is often used to characterize gas moving with the same bulk velocity. Clouds with line of sight velocity separations as small as 2.6 km s^{-1} have already been identified for the Procyon line of sight and smaller velocity separations may exist. High spectral resolution is also needed to measure line widths, which depend on temperature (T) and turbulent velocity (ξ) according to the relation $0.60 \times FWHM \approx b = \sqrt{0.0166T/A + \xi^2}$. This relation is valid for optically thin lines, where A is the atomic weight, ξ is the most probable speed of the turbulent mass motions (km s^{-1}), and b is the line width parameter, also in km s^{-1}. Measurement of the widths of the Mg II and Fe II lines (see Table I), which are needed to infer the value of ξ in a cloud, requires the resolution of the Goddard High Resolution Spectrograph (GHRS) echelles. High S/N is essential to measure the shapes of deep absorption features and especially the shape of the highly saturated H I Lyman-α interstellar absorption line. UV spectroscopy is needed because the column densities for short path lengths are very small, and resonance lines, typically found in the UV, are the most opaque lines for each ion.

Table I summarizes the capabilities of past, present, and future high-resolution UV spectrographs in space. Neither the Copernicus nor IUE spectrographs could resolve line profiles, and their low sensitivities hindered studies of weak lines, such as the important Lyman-α resonance line of D I, toward nearby stars. The echelle spectrographs on the GHRS (EA for short wavelengths and EB for longer wavelengths) have provided most of what we now know about the LISM, and

Space Science Reviews **78**: 157–164, 1996.

Table I
Comparison of High Resolution Spectroscopic Capabilities.

Satellite/ Instrument	Years Operational	Spectral Range (Å)	Spectral Resolution (km s^{-1})
Copernicus	1975 – 1979	900 – 3000	15
IUE/echelles	1978 –	1170 – 3400	25 – 30
HST/GHRS/EA	1990 – 1996*	1150 – 1730	3.57
HST/GHRS/G160M	1990 – 1996	1150 – 2300	20
HST/GHRS/G140M	1990 – 1996*	1100 – 1900	15
HST/GHRS/EB	1990 – 1996	1700 – 3200	3.54
HST/STIS/1.4	1997 –	1150 – 1700	2.9
HST/STIS/2.4	1997 –	1650 – 3100	2.9
HST/STIS/1.3	1997 –	1150 – 1700	12.5
HST/STIS/2.3	1997 –	1650 – 3100	12.8
FUSE	1998 –	900 – 1180	10 – 12

* Not operational in 1992 – 1994.
Typical value of $b_{\mathrm{H\ I}} = 11$ km s^{-1}.
Typical value of $b_{\mathrm{D\ I}} = 8$ km s^{-1}.
Typical value of $b_{\mathrm{Mg\ II}} = 2.6$ km s^{-1}.
Typical value of $b_{\mathrm{Fe\ II}} = 2.4$ km s^{-1}.

we anticipate that the echelles on the new Space Telescope Imaging Spectrograph (STIS) will extend this work by virtue of its large simultaneous spectral coverage to study many lines at one time. The Far Ultraviolet Spectrograph Explorer (FUSE) will permit studies of resonance lines of other ions (e.g., O VI, C III) at shorter wavelengths.

2. Kinematics of the LISM

Lallement and Bertin (1992) proposed that the Sun lies inside a cloud, which they called the Local Interstellar Cloud (LIC), because the line of sight velocities toward 6 nearby stars observed in ground-based Ca II spectra and the velocity of interstellar He I into the solar system are consistent with a single flow vector. GHRS spectra of the Mg II and Fe II resonance lines (2796, 2803, and 2600 Å) formed in the lines of sight toward other nearby stars (Lallement *et al.*, 1995) confirmed this picture with the flow vector magnitude 26 ± 1 km s^{-1} from Galactic coordinates $l = 186° \pm 3°$ and $b = -16° \pm 3°$ in the heliocentric rest frame. In the local standard of rest (defined by the motion of nearby stars), the LIC flow is from Galactic coordinates $l = 331.9°$ and $b = +4.6°$. The direction of this flow suggests that it originates from the expansion of a large superbubble created by supernovae and stellar winds from the Scorpius-Centaurus OB Association (Crutcher, 1982; Frisch, 1995).

GHRS spectra are confirming that the kinematical structure of the LISM is indeed very complex. Most lines of sight show at least one velocity component

in addition to the LIC, even for stars as close as Sirius (2.7 pc) and Procyon (3.5 pc), indicating that additional clouds lie outside of the LIC at short distances. Table II lists the number of clouds now identified on the lines of sight toward the stars observed with the GHRS, where L refers to the LIC. In the Galactic Center direction the Sun lies close to the edge of the G cloud as the α Cen stars show interstellar absorption only at the velocity of this cloud. The Sun likely lies very close to the edge of the LIC toward the North Galactic Pole as 31 Comae (Piskunov *et al.*, 1996) shows only one velocity component that is inconsistent with the LIC vector.

3. Physical Properties of the LISM

The temperature and nonthermal broadening of interstellar gas can be measured by comparing line widths of low mass elements (H and D) and high mass elements (e.g., Mg and Fe). For the line of sight to Capella, Linsky *et al.* (1995) derived $T = 7000 \pm 500 \pm 400$ K and $\xi = 1.6 \pm 0.4 \pm 0.2$ km s^{-1}, where the second uncertainty refers to the likely systematic errors in the uncertain intrinsic stellar emission lines. They also found $T = 6900 \pm 80 \pm 300$ K and $\xi = 1.21 \pm 0.27$ for the Procyon line of sight. Temperatures and turbulent velocities measured for other lines of sight through the LIC are consistent with these values. For example, Lallement *et al.* (1994) found that $T = 7600 \pm 3000$ K and $\xi = 1.4^{+0.6}_{-1.4}$ km s^{-1} for the LIC component toward Sirius, and Gry *et al.* (1995) found that $T = 7200 \pm 2000$ K and $\xi = 2.0 \pm 0.3$ km s^{-1} for the LIC component toward ϵ CMa. Recent analyses (Piskunov *et al.*, 1996) of the LIC components toward HR 1099, 31 Com, β Cet, and β Cas yield similar results, and *in situ* measurements of the LISM H I and He I atoms flowing through the heliosphere (cf. Lallement *et al.*, 1994) yield consistent values for the temperature. We therefore conclude that $T \approx 7000$ K and $\xi \approx 1.2$ km s^{-1} in the LIC.

Other clouds have different parameters. The G cloud, for example, is cooler with $T = 5400 \pm 500$ K and $\xi = 1.20 \pm 0.25$ km s^{-1} along the α Cen line of sight. Component 2 toward ϵ CMa is also cooler with $T = 3600 \pm 1500$ K and $\xi = 1.85 \pm 0.3$ km s^{-1} (Gry *et al.*, 1995) Hotter gas is inferred for several clouds toward ϵ CMa and for some of the gas toward Sirius (Bertin *et al.*, 1995).

Electron densities can be derived from the Mg II/Mg I column density ratio, assuming ionization equilibrium, but the derived densities are very temperature sensitive. For example, the ratio $R = N_{\rm Mg\ II}/N_{\rm Mg\ I} = 220^{+70}_{-40}$ for the Sirius line of sight (Lallement *et al.*, 1994) implies that $n_e = 0.3 - 0.7$ cm^{-3} if $T = 7000$ K and a much wider range for the plausible uncertainty in T. For the LIC component of the ϵ CMa line of sight, the measured ratio results in $n_e = 0.09^{+0.23}_{-0.07}$ cm^{-3} (Gry *et al.*, 1995) and a range in ionization fraction from nearly neutral to mostly ionized. For the LIC component of the Sirius line of sight, Frisch (1995) used both the Mg and C ionization fractions, which have opposite temperature dependencies,

to derive $n_e = 0.22 - 0.44$ cm^{-3}. Thus for $n_{\rm H\ I} = 0.1$ cm^{-3}, hydrogen in the LIC is mostly ionized with the photoionizing flux primarily from the star ϵ CMa.

4. The Three-Dimensional Structure of the LISM

The first attempts to map the distribution of interstellar gas in the solar neighborhood were based on measurements of $N_{\rm H\ I}$ extracted from Copernicus and IUE spectra primarily toward OB stars located near the Galactic plane. These maps (Frisch & York, 1983; Paresce, 1984) show a very asymmetric distribution of neutral hydrogen gas with the third Galactic quadrant (centered at $l = 225°$) showing the smallest column ($N_{\rm H\ I} \approx 5 \times 10^{18}$ cm^{-2}). This small column extends to at least 200 pc toward the star ϵ CMa (Gry *et al.*, 1995). GHRS spectra of some 19 mostly late-type stars now permit us to study the region within 20 pc of the Sun in more detail. These spectra sample lines of sight at Galactic latitudes from the North Galactic Pole (31 Com) to near the South Galactic Pole (β Cet), and they permit us to determine the amount of gas in each cloud along each line of sight.

Linsky, Piskunov, & Wood (1996) have created a three-dimensional morphological model for the LISM using the 12 lines of sight with Lα spectra listed in Table II and 5 additional lines of sight toward hot white dwarfs for which the analysis of EUVE spectra (Dupuis *et al.*, 1995) provide accurate estimates of the total value of $N_{\rm H\ I}$ (but no information on the specific clouds contributing to the H I column). Linsky *et al.* (1996) found that the LIC is flattened in the Galactic plane with minimum and maximum dimensions of about 1.6 and 4.8 pc, respectively. On the other hand, the total amount of warm gas in all clouds in the LISM is elongated roughly perpendicular to the plane with minimum and maximum dimensions of about 5.1 and 8.2 pc, respectively. These dimensions are based on the assumptions that the observed warm gas is located close to the Sun, can be approximated by a triaxial ellipsoid, and has a mean density of $n_{\rm H\ I} = 0.10$ cm^{-3}. The dimensions of the ellipsoids will scale inversely with the mean density. The direction of minimum hydrogen absorption through the LISM is near Galactic coordinates $l = 262°$ and $b = +22°$. They also find that $N_{\rm H\ I}$ is similar for stars located in the sky within 12°, which indicates that 12° is a typical angular scale of the clouds close to the Sun.

5. Discovery of Hydrogen Walls Around the Sun and Stars

Whereas the resonance lines of Mg II and Fe II are useful for studying clouds with $N_{\rm H\ I} \geq 10^{17}$ cm^{-2}, only the Lyman-α line of H I has sufficient opacity to study warm gas with columns as small as $N_{\rm H\ I} \approx 10^{13}$ cm^{-2}. For this reason and because of the uncertain shape of the intrinsic stellar emission line against which the interstellar absorption is measured, one must obtain Lyman-α line profiles with

Table II
Summary of GHRS Observations of the LISM.

Star (References)	d (pc)	l (°)	b (°)	Grating† (line)	Clouds in LOS	D/H (10^{-5})
α Cen A* [a,b]	1.3	316	–01	E(Lα,MgI+II,FeII)	G	
α Cen B [b]	1.3	316	–01	E(Lα,MgII)	G	
Sirius [a,c,d]	2.7	227	–09	G(Lα), E(MgI+II,FeII)	L+1	
ϵ Ind [e]	3.4	336	–48	E(Lα)	G?	1.6 ± 0.4
Procyon [f]	3.5	214	+13	G(Lα), E(MgII,FeII)	L+1	
α Aql [a]	5.0	48	–09	E(FeII,MgII)	L+2	
α PsA [a]	6.7	21	–65	E(FeII)		
Vega [a]	7.5	68	+19	E(FeII)	L+2	
β Leo [a]	12.2	251	+71	E(FeII,MgII)	L+2	
Capella* [f,g]	12.5	163	+05	E(Lα,MgII,FeII), G(Lα)	L	$1.60^{+0.14}_{-0.19}$
β Cas [h]	14	118	–03	G140M(Lα)	L	1.6 ± 0.4
β Cet [h]	16	111	–81	G(Lα), E(MgII)	L+1	2.2 ± 1.1
β Pic [a]	16.5	258	–31	E(FeII)	L	
λ And [e]	24	110	–15	E(Lα)	L+?	1.7 ± 0.5
δ Cas [a]	27	127	–02	E(MgII)	L	
HR1099* [h]	33	185	–41	E(Lα,MgII,FeII), G(Lα)	L+2	1.46 ± 0.09
G191-B2B [i]	48	156	+07	G(Lα), E(MgII,FeII)	L+2	$1.4^{+0.1}_{-0.3}$
31 Com [h]	80	115	+89	G(Lα), E(MgII)	1	1.5 ± 0.4
ϵ CMa [j]	187	240	–11	G(Lα), E(MgI+II,FeII)	L+5	

* These stars were observed twice. Capella and HR 1099 were observed near opposite quadratures.
† Gratings: G = G160M, E = Echelle-A or Echelle-B.
References: [a] Lallement *et al.* 1995, [b] Linsky & Wood 1996, [c] Lallement *et al.* 1994, [d] Bertin *et al.* 1995, [e] Wood *et al.* 1996, [f] Linsky *et al.* 1995, [g] Linsky *et al.* 1993, [h] Piskunov *et al.* 1996, [i] Lemoine *et al.* 1995, [j] Gry *et al.* 1995.

very high S/N and then analyze the data very carefully. Linsky and Wood (1996) therefore obtained high S/N GHRS spectra of two of the very nearest stars, α Cen A and α Cen B. They anticipated that the analysis of the Lyman-α lines toward these stars would be straightforward, as the line of sight is short (1.3 pc) and presumably simple. The intrinsic Lyman-α profile of α Cen A should be very similar to the Sun, as the two stars have the same spectral type, and the lines of sight to α Cen A and α Cen B (separated by only 20″) should have the same properties and thus provide redundant information.

Figure 1 shows the observed Lyman-α profile toward α Cen B and the best model fit in which the velocity and temperature of the interstellar H I are constrained to be the same as that obtained from the D I, Mg II, and Fe II lines. Clearly there is missing opacity near zero flux on the red side of the interstellar absorption, indicating additional absorption by gas that (i) is redshifted compared to the interstellar flow velocity of 18.0 km s^{-1}, (ii) is hotter that the interstellar gas (required to

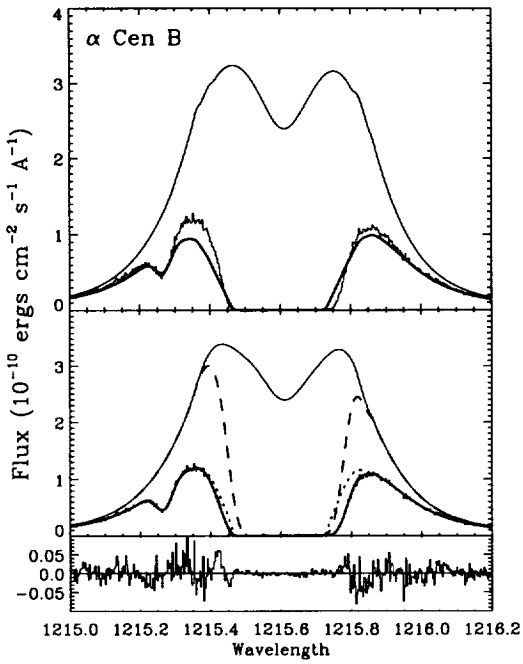

Figure 1. Upper panel: comparison of the observed Echelle-A spectrum (noisy line) of α Cen B with the assumed intrinsic stellar spectrum (smooth thin line) and the best one-component model fit (thick solid line). Middle panel: best two-component model with the absorption due to the ISM component only (dotted line), absorption due to the H wall component only (dashed line), and the total absorption (thick solid line). Lower panel: residuals between the observed profile and the two-component fit (from Linsky & Wood, 1996).

fit the gentler slope of the red side of the absorption compared to the blue side), and (iii) has a relatively low column density (the additional absorption has no Voigt wings). Because there is missing opacity at zero flux, no sensible change in the assumed intrinsic stellar profile can explain the discrepancy. Figure 1 also shows a least-squares fit to the observed profile by a two-component model. The second component gas is hot ($T = 29,000 \pm 5,000$ K), has a low column density ($\log N_{\rm H\,I} = 14.74 \pm 0.24$), and is redshifted by 2–4 km s^{-1} relative to the main component of the interstellar gas.

When Linsky and Wood (1996) derived these results they were unaware of the location of the second absorption component H I toward α Cen. The location became clear later at the 1995 July 12-13 meeting of the IUGG in Boulder, Colorado, where Baranov, Zank, and Williams presented their calculations of the interaction between the solar wind and the incoming interstellar flow. Their models (Baranov & Malama, 1993, 1995; Pauls *et al.*, 1995) which include charge

exchange between the outflowing solar wind protons and the inflowing H I atoms, show that near the heliopause there is a region of decelerated, hot hydrogen with higher density than in the LIC. This H I pileup region located about 200 AU in the upstream direction (depending on the proton density in the LIC) has been called the "hydrogen wall." Because the column density, temperature, and flow velocity of the H I agree well with the parameters derived for the second component toward α Cen, Linsky and Wood (1996) concluded that the second component originates in the wall. Before this time the hydrogen wall was just an interesting theoretical concept with no observational confirmation, although Lyman-α backscattering observations (e.g., Quémerais *et al.*, 1995) indicated that $n_{\mathrm{H\,I}}$ increases outward toward the heliopause.

Are there hydrogen walls around other stars? A stellar hydrogen wall would be seen as a second absorption component shifted to shorter wavelengths compared to the interstellar gas flowing toward the star, because the stellar wall would have to be viewed from the upwind direction. Wood, Alexander, & Linsky (1996) found that a one-component model for the interstellar absorption toward ϵ Ind could not explain the absorption on the blue side of the interstellar Lyman-α line. They concluded that a second component blueshifted by 18 ± 6 km s^{-1} with respect to the interstellar flow was needed with $\log N_{\mathrm{H\,I}} = 14.2 \pm 0.2$ and $T = 100,000 \pm 20,000$ K. The high temperature and large blueshift are consistent with the higher inflow velocity of 64.0 km s^{-1} toward this rapidly moving star. They also found evidence for a hydrogen wall around λ And with a smaller blueshift and temperature. Because the presence of a hydrogen wall requires a solar-like wind, the discovery of hydrogen walls around these two stars provides the first clear evidence that stars similar to the Sun actually have winds.

6. The D/H Ratio in the LISM

An important objective of the GHRS studies of nearby stars is to derive the D/H ratios along a number of lines of sight and to determine whether this ratio is constant in the LISM. The primordial value of D/H measures the baryon density of the universe and the parameter Ω_{B}, which is the ratio of the baryon density to the density needed to halt the expansion of the universe (the so called "closure density"). The value of D/H in the LISM is smaller than the primordial ratio because nuclear processes in stellar interiors destroy deuterium and stellar winds and supernova explosions eject deuterium-poor gas into the ISM. Comparison of hydrogen and deuterium column densities obtained from the same GHRS Lyman-α spectrum is a particularly good way to determine the D/H ratio, since in the warm absorbing gas H I and D I are the dominant stages of ionization with little association into molecules or depletion on to grains.

Table II summarizes the D/H ratios measured by various authors in the LIC component along different lines of sight (LOS). The measurements are all consistent

with a single value, $(1.6 \pm 0.2) \times 10^{-5}$. Thus the LISM appears to be well mixed on a time scale that is short compared to major perturbing events such as supernova explosions.

Acknowledgements

This work is supported by NASA through grant S-56460-D. The author thanks Brian Wood for creating the figure and ISSI for its hospitality and support.

References

Baranov, V. B., & Malama, Y. G.: 1993, *JGR*, **98**, 15,157.
Baranov, V. B., & Malama, Y. G.: 1995, *JGR*, **100**, A8, 14,755.
Bertin, P., Vidal-Madjar, A., Lallement, R., Ferlet, R., & Lemoine, M.: 1995, *A&A*, **302**, 889.
Crutcher, R.M.: 1982, *ApJ*, **254**, 82.
Dupuis, J., Vennes, S., Bowyer, S., Pradhan, A. K., & Thejll, P.: 1995, *Ap.J.*, **455**, 574.
Frisch, P. C.: 1995, *Science*, **265**, 1423.
Frisch, P. C., & York, D. G.: 1983, *Ap.J.*, **271**, L59.
Gry, C., Lemonon, L., Vidal-Madjar, A., Lemoine, M., & Ferlet, R., 1995, *A&A*, **302**, 497.
Lallement, R., & Bertin, P.: 1992, *A&A*, **266**, 479.
Lallement, R., Bertin, P., Ferlet, R., Vidal-Madjar, A., & Bertaux, J. L.: 1994, *A&A*, **286**, 898.
Lallement, R., Ferlet, R., Lagrange, A. M., Lemoine, M., & Vidal-Madjar, A.: 1995, *A&A*, **304**, 461.
Lemoine, M., Vidal-Madjar, A., Ferlet, R., Bertin, P., Gry, C., and Lallement, R.: 1995, in The Light Element Abundances, ed. P. Crane (Berlin; Springer), p. 233.
Linsky, J. L. & Wood, B. E.: 1996, *Ap.J.*, **462**, to appear May 20.
Linsky, J. L., Brown, A., Gayley, K., Diplas, A., Savage, B. D., Ayres, T. R., Landsman, W., Shore, S. N., & Heap, S. R.: 1993, *Ap.J.*, **402**, 694.
Linsky, J. L., Diplas, A., Wood, B. E., Brown, A., Ayres, T. R., & Savage, B. D.: 1995, *Ap.J.*, **451**, 335.
Linsky, J. L., Piskunov, N., & Wood, B. E.: 1996, submitted to *Science*.
Paresce, F.: 1984, *A.J.*, **89**, 1022.
Pauls, H. L., Zank, G. P., & Williams, L. L.: 1995, *JGR*, **100**, 21,595.
Piskunov, N., Wood, B., Linsky, J. L., Dempsey, R. C., & Ayres, T. R.: 1996, submitted to *Ap.J.*.
Quémerais, E., Sandel, B. R., Lallement, R., & Bertaux, J.-L.: 1995, *A&A*, **299**, 249.
Wood, B. E., Alexander, W. R., & Linsky, J. L.: 1996, *Ap.J.*, in press.